

Diffusion and MRI

Marta Morgado Correia

December 2, 2009

1 Introduction

Molecular diffusion refers to the random translational motion of molecules (also called Brownian motion) that results from the thermal energy carried by these molecules, a physical process that was well characterized by Einstein [1]. In a free medium, during a given time interval, molecular displacements obey a three-dimensional Gaussian distribution – molecules travel randomly in space over a distance that is statistically well described by a diffusion coefficient D . This coefficient depends only on the mass of the molecules, the temperature and the viscosity of the medium.

Diffusion MRI is deeply rooted in the concept that, during their diffusion driven displacements, molecules probe tissue structure on a microscopic scale, well beyond the usual (millimetric) image resolution. During diffusion, water molecules move inside the body, bouncing off, crossing or interacting with many tissue components, such as cell membranes, fibres and macromolecules. Because movement of water molecules is impeded by such obstacles, the actual diffusion distance is reduced compared with that of free water, and the displacement distribution is no longer Gaussian. In other words, although short diffusion times reflect the local intrinsic viscosity, at longer diffusion times the effects of the obstacles predominate. So, the non-invasive observation of water diffusion-driven displacement distributions in vivo provides unique clues to the fine structural features and geometric organization of neural tissues, and also to changes in these features with physiological and pathological states.

2 The Physics of Diffusion

The classical description of diffusion was introduced by Fick in the mid-1800's, with two differential equations that described diffusion macroscopically [2].

For an isotropic substance, Fick's first law states that the flux of particles across a membrane of unit area in a predefined plane, is proportional to the concentration differential across that plane:

$$\mathbf{F}(\mathbf{r}, t) = -D\nabla C(\mathbf{r}, t) \quad (1)$$

where \mathbf{F} is the flux of particles, C is their concentration, and D is the diffusion coefficient for that medium. When we combine this equation with the equation of conservation of mass:

$$\nabla \cdot \mathbf{F}(\mathbf{r}, t) = -\partial C(\mathbf{r}, t)/\partial t \quad (2)$$

we obtain Fick's second law:

$$D\nabla^2 C(\mathbf{r}, t) = \frac{\partial C(\mathbf{r}, t)}{\partial t} \quad (3)$$

The probability of finding a particle per unit volume is given by:

$$P(\mathbf{r}, t) = C(\mathbf{r}, t)/N \quad (4)$$

where N is the total number of particles in the system. Since N is a constant, $P(\mathbf{r}, t)$ obeys the same equation as $C(\mathbf{r}, t)$:

$$D\nabla^2 P(\mathbf{r}, t) = \frac{\partial P(\mathbf{r}, t)}{\partial t} \quad (5)$$

If at $t = 0$ a diffusing particle is known to be at position \mathbf{r}_0 , the probability of finding that particle at position \mathbf{r} at time t is found by solving equation (5) subject to the initial condition:

$$P(\mathbf{r}|\mathbf{r}_0, 0) = \delta(\mathbf{r} - \mathbf{r}_0) \quad (6)$$

In the case of unrestricted isotropic diffusion, this solution is given by:

$$P(\mathbf{r}|\mathbf{r}_0, t) = (4\pi Dt)^{-3/2} \exp \left\{ -\frac{1}{4Dt} |\mathbf{r} - \mathbf{r}_0|^2 \right\} \quad (7)$$

From equation (7) it can be observed that the probability density function $P(\mathbf{r}|\mathbf{r}_0, t)$ depends only on the displacement $\mathbf{r} - \mathbf{r}_0$, and not on the initial position, which reflects the Markov nature of Brownian motion [3]. Also, the Gaussian properties of $P(\mathbf{r}|\mathbf{r}_0, t)$ determine that the net molecular displacement at any time t is zero, whilst the mean square displacement, $\langle \Delta r \rangle^2$, is:

$$\langle \Delta r \rangle^2 = 2NDt \quad (8)$$

where $N = 1, 2$ or 3 , depending on whether the diffusion occurs in one (line), two (plane) or three (free space) dimensions, respectively. This relation for the mean square displacement during diffusion was first described by Einstein [1].

2.1 Anisotropic Diffusion

If the underlying brownian motion is not uniform in space, a single scalar diffusion coefficient can no longer describe the system completely. In this case, the flux of particles \mathbf{F} can be related to the concentration C via a diffusion tensor [4]:

$$\mathbf{F} = -\mathbf{D}\nabla C \quad (9)$$

where \mathbf{D} is a 3×3 matrix. Because diffusion has to be described by real values, this tensor is in fact symmetric ($D_{ij} = D_{ji}$) and it has only six independent elements:

$$\mathbf{D} = \begin{bmatrix} D_{xx} & D_{xy} & D_{xz} \\ D_{xy} & D_{yy} & D_{yz} \\ D_{xz} & D_{yz} & D_{zz} \end{bmatrix} \quad (10)$$

For a compartment with diffusion tensor \mathbf{D} , the probability that a particle initially at position \mathbf{r}_0 reaches position \mathbf{r} at time t is given by [8]:

$$P(\mathbf{r}|\mathbf{r}_0, t) = \frac{1}{\sqrt{|\mathbf{D}|(4\pi t)^3}} \exp \left\{ \frac{-(\mathbf{r} - \mathbf{r}_0)^T \mathbf{D}^{-1} (\mathbf{r} - \mathbf{r}_0)}{4t} \right\} \quad (11)$$

where $|\mathbf{D}|$ represents the determinant of \mathbf{D} .

3 Measuring Diffusion Using MRI

In MRI, the labelling of molecules is achieved via the characteristic Larmor frequencies of the component nuclei. The effects of diffusion on the spin echo signal were observed very early by Hahn [6] and later analysed by Carr and Purcell [9]. The attenuation of the spin echo signal resulting from the dephasing of the nuclear spins due to the combination of the translational motion of the spins and the imposition of spatially well defined gradient pulses can be used to measure motion. One of the most commonly used diffusion sensitising gradients is a modification of the spin echo sequence called pulsed gradient spin echo (PGSE), and was firstly introduced by Stejskal and Tanner [5]. This pulse sequence is shown in Figure 3.1.

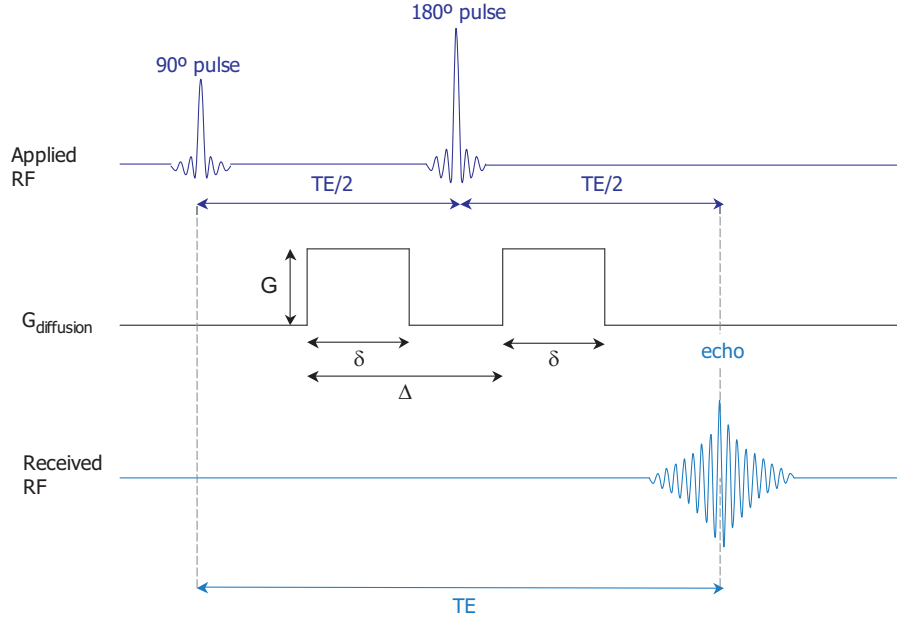


Figure 1: The Stejskal Tanner pulse sequence.

If a gradient pulse is introduced into the spin echo sequence after the 90° RF pulse, this will induce a phase shift $d(\phi_1)$ of the spin transverse magnetization, which depends upon the spin position. The phase shift introduced by a gradient applied along the z -axis is given by:

$$d(\phi_1) = \gamma \int_0^\delta G z dt = \gamma G \delta z_1 \quad (12)$$

where G is the gradient strength, δ its duration, and z_1 the position of the spins during the duration of the gradient, which is assumed to be constant during the short time δ . If an 180° RF pulse is applied afterwards, the phase shift is transformed into $-d(\phi_1)$. Hence, a second gradient pulse applied after the 180° RF pulse will cause another phase shift of contrary signal:

$$d(\phi_2) = \gamma \int_\Delta^{\Delta+\delta} G z dt = \gamma G \delta z_2 \quad (13)$$

where Δ is the diffusion time, which corresponds to the time between the two leading edges of the gradient pulses, and z_2 is the position of the spins during the second gradient pulse, in general different to z_1 due to the diffusion driven motion of molecules. The total phase shift would then be:

$$d(\phi) = \gamma G \delta (z_1 - z_2) \quad (14)$$

which means that if the labelled spins do not move (i.e., $z_1 = z_2$) the phase shift will be zero, whereas for the case where the spins have moved in time there is a phase shift that depends on the displacement ($z_2 - z_1$). The total magnetization of the spins is given by the sum of the magnetic moments:

$$\mathbf{M} = M_0 \sum_j \exp\{i d(\phi)_j\} \quad (15)$$

This summation can be calculated knowing the spin population. Therefore, the amplitude of the signal attenuation can be calculated using the following expression [10]:

$$\frac{S}{S_0} = \int \exp\{i \gamma G \delta (z_1 - z_2)\} P(z_2|z_1, \Delta) dz_2 \quad (16)$$

where S is the signal intensity, S_0 is the signal intensity in the absence of the diffusion weighting gradient, and $P(z_2|z_1, \Delta)$ is the probability of finding a spin initially at z_1 between the positions

z_2 and $z_2 + dz_2$, after a time Δ . If this equation is combined with the one-dimensional version of equation (7),

$$P(z_2|z_1, \Delta) = (4\pi D\Delta)^{-1/2} \exp \left\{ \frac{-(z_1 - z_2)^2}{4D\Delta} \right\} \quad (17)$$

the attenuation of the signal amplitude can be rewritten as:

$$\frac{S}{S_0} = \exp \left\{ -(\gamma G\delta)^2 \Delta D \right\} \quad (18)$$

The above equation is valid for finite ($\delta \ll \Delta$) and continuous gradients. In practice, diffusion gradient pulses have a certain length and are not applied continuously, hence, the more general approach given by Stejskal and Tanner should be used [5]:

$$\frac{S}{S_0} = \exp \left\{ -\gamma^2 D \left(\int_0^{2\tau} F^2 dt - 4f \int_{\tau}^{2\tau} F dt + 4f^2 \tau \right) \right\} \quad (19)$$

where 2τ is the time at the centre of the echo (TE), τ the time at the centre of the 180° pulse, $F(t)$ is a phase function that depends on the gradients applied,

$$F(t) = \int_0^t G(t') dt', \quad (20)$$

f is the phase function $F(t)$ evaluated at τ , and $G(t')$ is the gradient strength at time t' . If equation (19) is solved for the pulse sequence shown in Figure 3.1, the solution is:

$$\frac{S}{S_0} = \exp \left\{ -\gamma^2 G^2 \delta^2 \left(\Delta - \frac{1}{3} \delta \right) D \right\} \quad (21)$$

This equation can be rearranged to give:

$$S = S_0 e^{-bD} \quad (22)$$

where b is the so-called b-value, and is defined by:

$$b = \gamma^2 G^2 \delta^2 \left(\Delta - \frac{1}{3} \delta \right) \quad (23)$$

The b-value has units of s/mm^2 and represents the sensitivity of the sequence to motion, i.e., the greater the b-value, the greater the diffusion weighting of the image.

In the case of anisotropic diffusion, Bassler *et al* [7] derived a formula analogous to that proposed by Stejskal and Tanner [5], where the signal attenuation is related to the diffusion tensor, \mathbf{D} , by:

$$S = S_0 e^{-\mathbf{B}:\mathbf{D}} \quad (24)$$

where \mathbf{B} is the so-called b-matrix:

$$\mathbf{B} = \begin{bmatrix} B_{xx} & B_{xy} & B_{xz} \\ B_{xy} & B_{yy} & B_{yz} \\ B_{xz} & B_{yz} & B_{zz} \end{bmatrix} \quad (25)$$

More details on the b-matrix and the diffusion tensor experiment will be provided in section 3.3.

In the case of an anisotropic diffusion profile, equation (22) can still be used to estimate the average diffusivity along the acquired gradient direction. In this case, the diffusion coefficient, D , is replaced by the concept of apparent diffusion coefficient, ADC.

3.1 Twice Refocused Spin Echo

One of the main sources of artifacts in diffusion-weighted MRI images is the presence of eddy currents. The time-varying magnetic fields from gradients in MRI pulse sequences induce currents in conducting structures within the magnet, gradient coils themselves, and RF coils [11]. The induced currents are called eddy currents, and create unwanted magnetic fields that are detrimental to image quality.

In order to minimise the effects of eddy currents, for our data acquisition we used the twice refocused spin echo (TRSE) pulse sequence proposed by Reese and colleagues [12]. This sequence is shown in Figure 3.2.

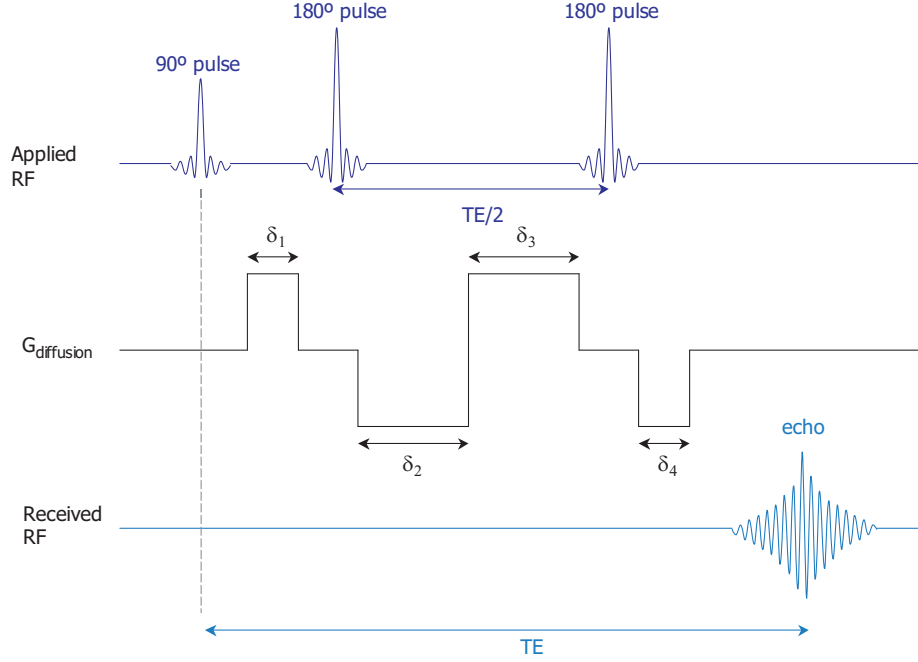


Figure 2: The TRSE pulse sequence.

The TRSE pulse is formed by an SE diffusion sequence with two refocusing pulses. Two bipolar field gradients of length $\delta_1 + \delta_2$ and $\delta_3 + \delta_4$ are used, with the RF refocusing pulses dividing each bipolar pair. If we consider an idealised sequence, in which the RF pulse durations and gradient ramping times are infinitely short, then:

$$\begin{aligned} \delta_1 + \delta_2 &= \delta_3 + \delta_4 \\ \delta_2 + \delta_3 &= TE/2 \\ \delta_1 + \delta_4 &= TE/2 - t_{pr} \end{aligned} \quad (26)$$

where t_{pr} is the sum of the preparation time following the excitation pulse and the readout time preceding the SE. Three equations for four unknowns, leaves one free parameter. For a Siemens 3T Trio, the following additional equations are used to obtain unique solutions for the unknown timing values:

$$\begin{aligned} t_{diff} &= \delta_1 + \delta_2 + \delta_3 + \delta_4 \\ TE &= t_{pr} + t_{diff} \\ e^{-\lambda T} - 2e^{-\lambda(T-\delta_1)} + 2e^{\lambda(T-\delta_1-\delta_2)} - 2e^{\lambda(T-\delta_1-\delta_2-\delta_3)} + e^{\lambda(T-\delta_1-\delta_2-\delta_3-\delta_4)} &= 0 \end{aligned} \quad (27)$$

where t_{diff} is the time available for diffusion weighting, and T is the total time from the first gradient rise to echo. λ is the time constant associated to the eddy current decay, and its value is set by the scanner.

Eddy currents are created by gradient slewing, and are roughly proportional to the slew duration and rate, which is in turn equal to the amount of change in the gradient amplitude. When gradient

waveforms are a trapezoid, eddy currents caused by the initial and final (positive and negative) ramps tend to cancel each other out, if they are close [13]: this is the effective utility of split diffusion gradients.

3.2 Noise in MRI images

The data acquired to form an MRI image contain noise, which is introduced in the acquisition phase by the MR hardware. This noise is assumed to be random, and following a Gaussian distribution with zero mean, and standard deviation σ [14]. The noise from the acquisition is retained in the actual image through the Fourier transform process, since the Fourier transform is a linear and orthogonal operator. However, the images commonly used in MRI are normally magnitude images, which are obtained by calculating the magnitude value of the complex image on a voxel by voxel basis. This process alters the properties of the noise distribution, making it no longer Gaussian. Instead, the noise is now characterised by a Rician distribution [15]. If A is the true signal intensity of a voxel in the absence of noise, and M is the measured voxel intensity, the distribution of M is given by:

$$P_M(M) = \frac{M}{\sigma^2} e^{-\frac{M^2+A^2}{2\sigma^2}} I_0\left(\frac{A M}{\sigma^2}\right) \quad (28)$$

where I_0 is the modified zeroth order Bessel function of the first kind.

For high signal-to-noise ratio (SNR), the Rician distribution can be well approximated by a Gaussian, but the same is not true for lower levels of SNR.

3.3 The Diffusion Tensor Model

MRI can measure molecular diffusion along any desired directional axis by using three independent gradient units that are orthogonal to each other: x , y , and z . When water is freely diffusing, its diffusion is isotropic and the diffusion coefficient D is a constant, since it does not depend on the direction of the applied gradient. However, water in living systems is often contained in very ordered structures that restrict its diffusion along certain axes. For example, consider a water molecule confined to move inside a cylindrical shaped tube along the z -axis. In this case, a diffusion constant measured along the z -axis is larger than those along x and y .

In practice, highly ordered biological structures do not usually align with the physical coordinates x , y and z defined by the orientation of an MRI scanner. In this case, what we measure using x , y and z gradients is diffusion along an oblique angle with respect to the ordered structure.

As discussed in the previous sections, to fully characterise an anisotropic diffusion profile we can use a 3×3 tensor, called the diffusion tensor (DT) (see equation (10)). When a diffusion measurement is made along the x , y or z axis, what we measure is D_{xx} , D_{yy} and D_{zz} , respectively.

The meaning of this diffusion tensor can be more easily understood using the so-called diffusion ellipsoids (Figure 3.3). In an isotropic environment, the diffusion tensor has only diagonal elements (D_{xx} , D_{yy} and D_{zz}), all of which have the same value. Thus, the system can be characterized by only one constant, D , and the diffusion ellipsoid is spherical (the radius of the sphere is proportional to \sqrt{D}). In an anisotropic environment, the ellipsoid is elongated. We call the longest, middle and shortest axes of this ellipsoid principal axes, and the three diffusion coefficients along these axes λ_1 , λ_2 and λ_3 . When the principal axes happen to align to our physical coordinates x , y and z , we can directly measure λ_1 , λ_2 and λ_3 . In practice, they are almost never aligned and the diffusion tensor has nine non-zero elements. Because D_{xx} , D_{yy} and D_{zz} values change as the orientation of the object changes, so does the measured diffusion constant using x -, y - or z -gradient axes.

In section 3, we introduced the b-matrix, \mathbf{B} , to describe the coupling between the diffusion tensor elements and the signal attenuation, for a given gradient direction, amplitude, duration, and separation. The components of the b-matrix are given by [16]:

$$\mathbf{B} = \begin{bmatrix} br_x^2 & br_x r_y & br_x r_z \\ br_x r_y & br_y^2 & rr_y r_z \\ br_x r_z & br_y r_z & br_z^2 \end{bmatrix} \quad (29)$$

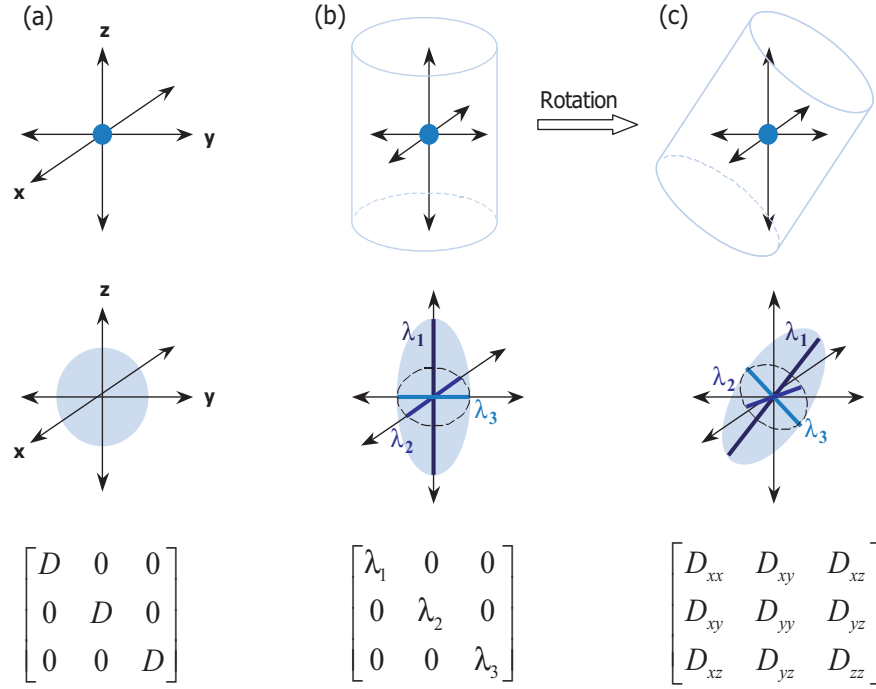


Figure 3: Relationship between anisotropic diffusion (upper row), diffusion ellipsoids (middle row) and diffusion tensor (bottom row). (a) Isotropic diffusion – water diffuses equivalently in all directions. (b),(c) Anisotropic diffusion – water diffusion has directionality.

where $\mathbf{r} = (r_x, r_y, r_z)$ is the gradient direction, and b is the b-value as defined in equation (23). Equation (24) can now be rewritten as:

$$S(b, \mathbf{r}) = S_0 e^{-br_x^2 D_{xx} - br_y^2 D_{yy} - br_z^2 D_{zz} - 2br_x r_y D_{xy} - 2br_x r_z D_{xz} - 2br_y r_z D_{yz}} \quad (30)$$

which can be rearranged further to give:

$$S(b, \mathbf{r}) = S_0 e^{-b\mathbf{r}^T \mathbf{D} \mathbf{r}} \quad (31)$$

A minimum of six non-collinear diffusion measurements is required to fully estimate the diffusion tensor. To eliminate the dependence of spin density, T_1 and T_2 we must take at least two measurements of diffusion-weighted images that are differently sensitised to diffusion (different b-values), but remain identical in all other respects. The more traditional approach is to acquire one image without diffusion weighting ($b=0$), the baseline image, and use a second value of b for the six non-collinear acquisitions. However, a higher number of directions and b-values can be used to improve the accuracy of the estimated tensor.

From equation (31) we see that the signal is comprised of exponentially weighted projections of the diffusion tensor. The projected diffusion values in the measurement space are equivalent to:

$$D_m(\mathbf{r}) = \mathbf{r}^T \mathbf{D} \mathbf{r} = \frac{\ln S_0 - \ln S(b, \mathbf{r})}{b} \quad (32)$$

By measuring D_m with high angular resolution sampling, the shape of the diffusion measurement profile as a function of \mathbf{r} can be determined. If we express D_m as the radius from the origin as a function of the spherical coordinates (θ, ϕ) ¹, we obtain the “peanut-shaped” surfaces shown in Figure 3.4.

¹Note that any direction \mathbf{r} can be represented by the spherical coordinates (θ, ϕ) : $\mathbf{r} = (\sin \theta \cos \phi, \sin \theta \sin \phi, \cos \theta)$.



Figure 4: The measured diffusivity, D_m , as a function of the spherical coordinates (θ, ϕ) for two identical cylindrically symmetric fibres ($\lambda_1 = 1.4 \text{ mm}^2/\text{s}$, $\lambda_2 = \lambda_3 = 0.35 \text{ mm}^2/\text{s}$) oriented 90° to one another. These plots were obtained using Matlab 7 (Mathworks Inc., Natick, MA).

3.4 Parameters Derived from the Diffusion Tensor

Measurements of the diffusion tensor and its components have been found to have several applications in the human brain [17, 18]. The trace of the diffusion tensor:

$$\text{trace}(\mathbf{D}) = D_{xx} + D_{yy} + D_{zz} = \lambda_1 + \lambda_2 + \lambda_3 \quad (33)$$

has been found to be valuable for detecting and evaluating brain ischemia and stroke [19, 20]. Frequently, the mean diffusivity (MD) is used instead of $\text{trace}(\mathbf{D})$:

$$\text{MD} = \frac{\text{trace}(\mathbf{D})}{3} = \frac{\lambda_1 + \lambda_2 + \lambda_3}{3} = \langle \lambda \rangle \quad (34)$$

In the context of diffusion tensor imaging, the concepts of mean diffusivity and apparent diffusion coefficient (ADC) are often used interchangeably in the literature, although ADC strictly refers to the diffusion coefficient along a particular direction.

Measures of diffusion tensor anisotropy have been used to study white matter in terms of morphology [21], disease and trauma [22, 23] and brain development [24, 25]. The most commonly used index of anisotropy is the fractional anisotropy (FA) [26] and is defined as:

$$\text{FA} = \sqrt{\frac{3((\lambda_1 - \langle \lambda \rangle)^2 + (\lambda_2 - \langle \lambda \rangle)^2 + (\lambda_3 - \langle \lambda \rangle)^2)}{2(\lambda_1^2 + \lambda_2^2 + \lambda_3^2)}} \quad (35)$$

FA measures the fraction of the “magnitude” of \mathbf{D} that can be ascribed to anisotropic diffusion. For an isotropic medium, $\text{FA} = 0$. For an infinitely anisotropic medium (i.e., $\lambda_2 = \lambda_3 = 0$), $\text{FA} = 1$. Images of the FA index are bright in regions where there are anisotropic structures and dark in more isotropic regions.

Based on the eigenstructure of the measured diffusion tensor it is also possible to infer the orientation of the diffusion compartments within the voxel: the major eigenvector of the diffusion tensor is parallel to the mean fibre orientation [27] and the minor eigenvector parallels the normal to the mean plane of fibre dispersion [28]. More recently, several investigators proposed using the principal eigenvectors of the diffusion tensor to estimate white matter connectivity [29–31].

Using conventional MRI we can easily identify the different structures of the brain. However, in these images the white matter of the brain appears to be homogeneous without any suggestion of the complex arrangement of fibre tracts. On the other hand, the MRI measurements of \mathbf{D} in tissues can provide unique biologically and clinically relevant information that is not available from other imaging modalities. This information includes parameters that help characterize tissue composition, the physical properties of tissue constituents and its architectural organization. Moreover, this measurement is performed noninvasively, without exogenous contrast agents.

References

- [1] Einstein A. Investigations on the theory of Brownian Motion. Dover, New York, 1956.

- [2] Fick A. On liquid diffusion. *Philosoph Mag* 10: 30-39, 1855.
- [3] Callaghan P. *Principles of Nuclear Magnetic Resonance Microscopy*. Clarendon Press, Oxford, 1991.
- [4] Crank J. *The Mathematics of Diffusion*. Oxford University Press, 1956.
- [5] Stejskal EO, Tanner JE. Spin diffusion measurements: spin echoes in the presence of time-dependent field gradient. *J Chem Phys* 42: 292-299, 1965.
- [6] Hahn EL. *Phys Rev* 80: 288-292, 1950.
- [7] Basser PJ, Mattiello J, LeBihan D. Estimation of the effective self-diffusion tensor from the NMR spin echo. *J Magn Reson, Series B* 103:247-254, 1994.
- [8] Basser PJ, Mattiello J, Le Bihan D. MR diffusion tensor spectroscopy and imaging. *Biophys J* 66: 259-267, 1994.
- [9] Carr H, Purcell E. Effects of free precession in nuclear magnetic resonance experiments. *Physical Review* 94: 630-638, 1954.
- [10] Le Bihan D, Mangin J, Poupon C, Clark C, Pappata S, Molko N, Chabriat H. Diffusion tensor imaging: Concepts and Applications. *J Magn Reson Imag* 13: 534-546, 2001.
- [11] Bernstein MA, King KF, Zhou XJ. *Handbook of MRI Pulse Sequences*. Elsevier, USA, 2004.
- [12] Reese TG, Heid O, Weisskoff RM, Wedeen VJ. Reduction of eddy-current-induced distortion in diffusion MRI using a twice-refocused spin-echo. *Magn Reson Med* 38: 638-644, 2003.
- [13] Johansen-Berg H, Behrens TEJ. *Diffusion MRI: From quantitative measurement to in vivo neuroanatomy*. Elsevier, USA, 2009.
- [14] Henkelman RM. Measurement of signal intensities in the presence of noise in MR images. *Medical Physics* 12: 232-233, 1985.
- [15] Gudbjartsson H, Patz S. The Rician distribution of noisy MRI data. *Magn Reson Med* 34: 910-914, 1995.
- [16] Mattiello J, Basser PJ, Le Bihan D. The b-matrix in diffusion tensor echo-planar imaging. *Magn Reson Med* 37: 292-300, 1997.
- [17] Peled S, Gudbjartsson H, Westin CF, Kikinis R, Jolesz FA. Magnetic resonance imaging shows orientation and asymmetry of white matter fibre tracts. *Brain Res* 780: 27-33, 1998.
- [18] Pierpaoli C, Jezzard P, Basser PJ, Barnett A, Di Chiro G. Diffusion tensor MR imaging of the human brain. *Radiology* 201: 637-648, 1996.
- [19] Moseley ME, Butts K, Yenari MA, Marks M, de Crespigny A. Clinical aspects of DWI. *NMR Biomed* 8: 387-396, 1995.
- [20] Warach S, Gaa J, Siewert B, Wielopolski P, Edelman RR. Acute human stroke studied by whole brain echo planar diffusion-weighted magnetic resonance imaging. *Ann Neurol* 37: 231-241, 1995.
- [21] Makris N, Worth A, Sorensen A, Papadimitriou G, Wu O, Reese T, Wedeen V, Davis T, Stakes J, Gaviness V, Kaplan E, Rosen B, Pandya D, Kennedy D. Morphometry of in vivo human white matter association pathways with diffusion-weighted magnetic resonance imaging. *Ann Neurol* 42: 951-962, 1997.

- [22] Brunberg JA, Chenevert TL, McKeever PE, Ross DA, Junck LR, Muraszko KM, Dauser R, Pipe JG, Betley AT. In vivo MR determinations of water diffusion coefficients and diffusion anisotropy: correlation with structural alteration in gliomas of the cerebral hemispheres. *AJNR Am J Neuroradiol* 16: 361-371, 1995.
- [23] Werring DJ, Clark CA, Barker GJ, Miller DH, Parker GJ, Brammer MJ, Bullmore ET, Giampietro VP, Thompson AJ. The structural and functional mechanisms of motor recovery: complementary use of diffusion tensor and functional magnetic resonance imaging in a traumatic injury of the internal capsule. *J Neurol Neurosurg Psychiatry* 65: 863-869, 1998.
- [24] Neil JJ, Shiran SI, McKinstry RC, Schefft GL, Snyder AZ, Almlie CR, Akbudak E, Aronovitz JA, Miller JP, Lee BC, Conturo TE. Normal brain in human newborns: apparent diffusion coefficient and diffusion anisotropy measured by using diffusion tensor MR imaging. *Radiology* 209: 57-66, 1998.
- [25] Huppi PS, Maier SE, Peled S, Zientara GP, Barnes PD, Jolesz FA, Volpe JJ. Microstructural development of human newborn cerebral white matter assessed in vivo by diffusion tensor magnetic resonance imaging. *Pediatr Res* 44: 584-590, 1998.
- [26] Basser PJ, Pierpaoli C. Microstructural and physiological features of tissues elucidated by quantitative diffusion tensor MRI. *J Magn Reson Series B* 111: 209-219, 1996.
- [27] Basser PJ, Mattiello J, LeBihan D. MR diffusion tensor spectroscopy and imaging. *Biophys J* 74: 789-793, 1994.
- [28] Wiegell MR, Larsson HB, Wedeen VJ. Fiber crossing in human brain depicted with diffusion tensor MR imaging. *Radiology* 217: 897-903, 2000.
- [29] Poupon C, Mangin J, Frouin V, Regis J, Poupon F, Pachot-Clouard M, Le Bihan D, Bloch I. Regularization of MR diffusion tensor maps for tracking brain white matter bundles. In: *Medical image computing and computer-assisted intervention MICCAI*. Berlin: Springer Verlag 489-498, 1998.
- [30] Mori S, Crain BJ, Chacko VP, van Zijl PC. Three-dimensional tracking of axonal projections in the brain by magnetic resonance imaging. *Ann Neurol* 45: 265-269, 1999.
- [31] Conturo TE, Lori NF, Cull TS, Akbudak E, Snyder AZ, Shimony JS, McKinstry RC, Burton H, Raichle ME. Tracking neuronal fibre pathways in the living human brain. *Proc Natl Acad Sci USA* 96: 10422-10427, 1999.